Available online at www.sciencedirect.com
ScienceDirect
European Journal of Mechanics B/Fluids 25 (2006) 574–585

Three reasons for freak wave generation in the non-uniform current

I.V. Lavrenov [a,*], A.V. Porubov [b]

[a] *Arctic and Antarctic Research Institute, St. Petersburg, Russia*
[b] *A.F. Ioffe Physical Technical Institute, St. Petersburg, Russia*

Received 17 October 2005; received in revised form 10 February 2006; accepted 24 February 2006

Available online 5 June 2006

Abstract

Three reasons for freak wave generation due to interaction of wave with spatially non-uniform current are considered in the paper. They are as follows: wave energy amplification due to wave-current interaction; wave height amplification around caustic due to refraction wave in non-uniform current; non-linear wave interaction in shallow water due to their intersection described by the Kadomtsev–Petviashvili equation. These mechanisms can generate a large wave amplification producing a dangerous natural phenomenon.

Keywords: Freak wave; Non-uniform current; Wave-current interaction; Non-linear waves

0. Introduction

During last years considerable attention has been paid to investigation of freak wave as a phenomenon producing dangerous impact on ships and oil platforms in seas. According to the modern definition, this phenomenon is a wave with height being larger than 2.2 times of significant wave height value. In fact, as soon as wind wave height distribution is approximated by the Rayleigh distribution with sufficient accuracy, it allows getting any wave height value with an appropriate probability. It means that the wave height with the value larger than 2.2 times of significant value can be found in any wave record. It becomes obvious that in case of a freak wave, as a dangerous natural phenomenon, such definition is not sufficient.

It should be noted that originally the term ‘freak waves’ (or abnormal waves, exceptional waves, killer waves, cape roller and rogue waves) pertains to individual asymmetric waves with a crest of an extremely high slope, in front of which there appears a longer and deeper trough than compared with ordinary wind waves. This trough looks like a hole in the sea. It is rather difficult to observe a hole at some distance from a ship. However, the total height of such waves can reach 15–20 m and more, sometimes in a relatively calm sea. Waves often appear suddenly. That is why it is practically impossible for a ship’s crew to take any precaution measures.

Abnormal waves are observed frequently in different regions of the world ocean, where there are strong currents: for example, Gulfstream, Kuroshio and others. Extremely large waves are observed near the southeastern shore of South

* Corresponding author.
E-mail address: lavren@aari.nw.ru (I.V. Lavrenov).

0997-7546/$ – see front matter
doi:10.1016/j.euromechflu.2006.02.009

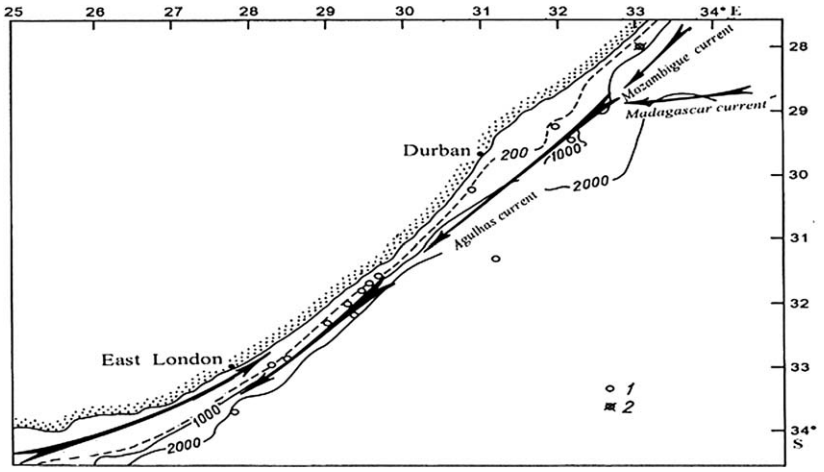

Fig. 1. Map of the Southeast Coast (South Africa). 1 – location abnormal wave accidence; 2 – location of the "Taganrogsky zaliv" tanker-refrigerator.

Africa in the Agulhas current between East London and Durban (Fig. 1). That is why the region is considered to be very dangerous. A list of cases when abnormal waves were observed up to 1973 is presented by captain Mallory [1], along with an analysis of the corresponding atmospheric and oceanographic conditions, which were responsible to a great extent for the appearance of the abnormal waves. In his article, captain Mallory showed 11 cases of catastrophic ship collisions with abnormal waves in the region (Fig. 1). The conditions mainly come down to the conjunction of the southwesterly waves with the passage of an atmospheric cold front. In fact, abnormal waves appeared here more often and the consequences of their action were less dramatic. It can be explained by weather conditions of the area when ships had to slow down their speed and diminish the effect of the wave action.

On April 27, 1985 at 01.01 p.m. ship time (11.01 a.m. GMT), the Soviet tanker-refrigerator "Taganrogsky Zaliv"[1] was subjected to the abnormal wave (the point of accident is denoted by a circle with a cross in Fig. 1). As a result, a sailor working on a foredeck was mortally wounded and washed overboard.

That time one of the authors of this paper was invited as a wind wave expert to take part in the work of the Commission of the Crimean Transport Prosecuting Office, examining the incident [2]. As a result of the Commission's investigations, a number of peculiar details concerning abnormal wave generation were revealed. They were used later in mathematical modeling of this phenomenon.

On date under discussion, the "Taganrogsky Zaliv" tanker-refrigerator was sailing from the Indian Ocean to the Southeast Atlantic. The possibility of encountering a weather storm is high enough near the Cape of Good Hope. That is why the ship was prepared for sailing in stormy weather. The north-north east wind was blowing at a speed of 7 m s^{-1}. At 5 a.m., it changed its direction to south-south west with the same force. From the previous day the atmospheric pressure was diminishing until the wind changed direction, after that it began increasing. At 8.00 a.m., the wind became stronger and at 11.00 a.m. it reached 15 m s^{-1}. After 12.00, the wind speed diminished to 12 m s^{-1}. Sea wind became calmer. The wind force did not change during the next three hours. Wave height did not exceed 5m and the length was 40–45 m. The weather conditions were suitable for performing deck reparation works. The location of the ship is shown by cross in Fig. 1 [2]. About 13.00 the front part of the ship suddenly dipped, and the crest of a very large wave appeared close to the foredeck. Wave crest reached value 5–6 m higher over the foredeck. The wave crest fell down on the ship. One of the seamen was killed and washed overboard. All attempts to save him were in vain. Nobody was able to foresee the appearance of such a wave. When the ship went down, riding on the wave, and its frontal part was stuck into water, nobody felt the wave's impact. The wave easily rolled over the foredeck, covering it with more than two meters of water (see Fig. 2). The length of the wave crest was not more than 20 m. Accident of freak wave impact of the ship is presented in Fig. 2 according to ship's crew description.

[1] "Taganrogsky zaliv" is a ship of the unrestricted sailing radius. The vessel length is 164.5 m, the largest width is 22 m, the displacement during accident was 15 000 ton, the board height above water was 7 m.

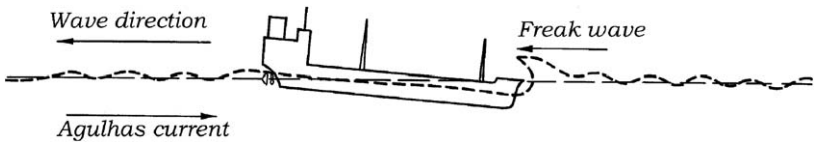

Fig. 2. Rogue (freak) wave attack on the ship.

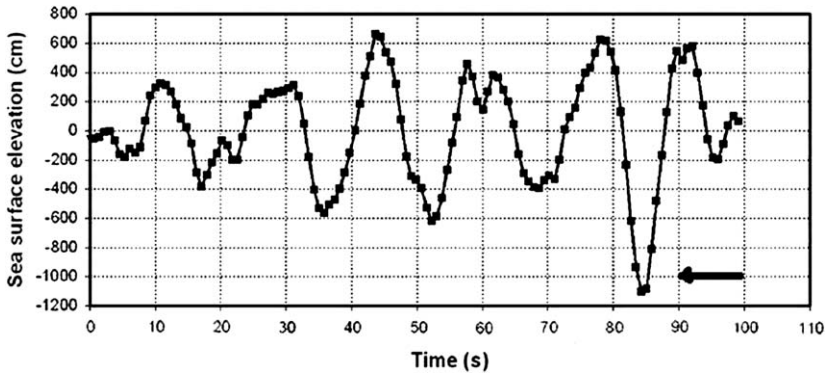

Fig. 3. Observation of a hole near the South Africa coast. Abnormal hole is marked by an arrow.

The unusual wave looked like a deep hole in the sea, which appeared so suddenly in front of the ship that it was practically impossible to make any precaution measures to avoid ship's sliding down into deep wave trough.

Recently another abnormal waves with deep trough were registered in the ocean. Such a wave was observed near the South Africa coastal zone, where the ocean depth was 70 m [3]. It looks like the usual envelope wave but for the part with deep trough marked by an arrow in Fig. 3. Its magnitude A is equal to $A = 11$ m while the neighboring crests are not higher than 6 m. The speed of the wind was about $U_0 = 30$ m/sec. In this case the velocity of the wind turns out about the velocity of the linear surface waves in limited depth $\sqrt{gH}$.

Nowadays there are a lot of different results devoted to the freak wave investigation. Detailed overview is published by Kharif and Pelinovsky [4]. It should be noted that the main attention in almost all papers is paid to the study of generation wave with a large crest. At the same time there is lack of results devoted to the generation of wave with deep trough (WWDT) in the sea.

From the point of view of the linear theory the probability observing wave with large crest is the same as for wave with deep trough. On the other hand, from the non-linear surface wave theory (at least for Stokes wave theory or solitary wave in shallow water) the value of crest is larger than value of trough depending on wave steepness.

There is a question what kind of physical mechanisms can be responsible for generation of waves with deep trough (WWDT) in the sea.

Starting from the water wave theory it is hardly possible to suppose obtaining a soliton solution for WWDT. However, other mechanisms of the freak wave generation can be applied for explanation of the WWDT generation in the sea. So, the following mechanisms should be mentioned:

- Wave transformation in non-uniform current [2,5];
- Dispersion focusing [4,6], as soon as it can be based on linear theory;
- Non-linear wave modulation [6] based on the Schrödinger equation;
- Wave refraction due to uneven bottom [4];
- Spatial non-uniform and/or temporal non-steady wind field [2,5];

In the present paper, main attention will be paid to the problem of the wave transformation in non-uniform current, which can produce WWDT. In turn, there are at least three reasons for freak wave generation in non-uniform current. They can be mentioned as follows:

- Wave energy amplification due to wave-current interaction;
- Wave height amplification around caustic due to refraction wave in non-uniform current;
- Non-linear wave interaction in shallow water due to their intersection described by KP equation.

The idea is to overview our recent works and to bring together main findings in order to illustrate and justify above mentioned reasons.

1. Wave energy amplification due to wave-current interaction

As it is shown above, the wave interaction with spatially non-uniform current could provide a necessary condition for freak wave generation. A large wave appearance in the Agulhas current can be explained by a local wave pattern generated by wave reflection from the current. The abnormal waves are typically observed on the oceanic surface, where the depth approximately coincides with a 200-m isobath. The latter passes parallel to the coastline. It is the boundary of the continental shelf, where the depth increases sharply to 3–4 km (see Fig. 1). The sharp depth variation at the continental shelf margin results in the maximum values of the Agulhas current, having a jet profile directed parallel to the shoreline. The transversal profile of the Agulhas current velocity distribution is not changed much along its entire length from the Mozambique and South Madagascar current confluence at the latitude 30 degree South (see Fig. 1). The typical horizontal profile of the current velocity distribution in the transversal direction [7] is presented in Fig. 4. The axis Ox of the co-ordinate system is chosen along the current velocity direction, and the axis Oy is in the perpendicular one.

A transversal profile of the current velocity $\boldsymbol{V} = \{V_x(y), 0\}$ in this area can be quite accurately approximated using the relation:

$$V_x = \frac{b_1}{1 + b_2 y^2}, \tag{1.1}$$

where $b_1 = 2.2\ \mathrm{m\,s^{-1}}$, $b_2 = 6.25 \times 10^{-10}\ \mathrm{m^{-2}}$ at $y < 0$, $b_2 = 10^{-8}\ \mathrm{m^{-2}}$ at $y > 0$.

The current velocity distribution (1.1) is assumed to be valid at $x < 0$ in the chosen co-ordinate system. The point $\{x = 0, y = 0\}$ is assumed to be correspondent to the current velocity midstream at the point with co-ordinates $\{27^\circ\ \mathrm{E}, 34^\circ\ \mathrm{S}\}$.

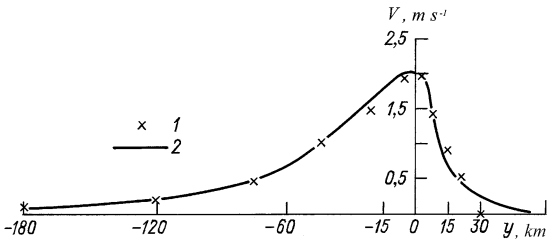

Fig. 4. Distribution of horizontal current velocity in transversal direction. 1 – velocity values according to Schumann [7]; 2 – approximation (1).

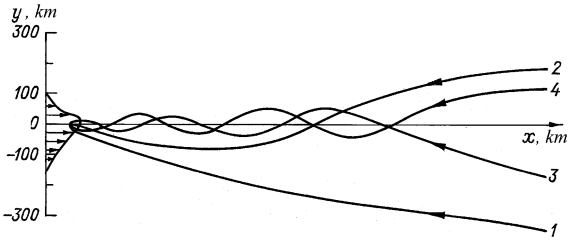

Fig. 5. Wave rays in jet current arriving to the given point with frequency ω: $1 - 0.20\ \mathrm{rad\,s^{-1}}$, $2 - 0.38\ \mathrm{rad\,s^{-1}}$, $3 - 0.76\ \mathrm{rad\,s^{-1}}$, $4 - 0.93\ \mathrm{rad\,s^{-1}}$.

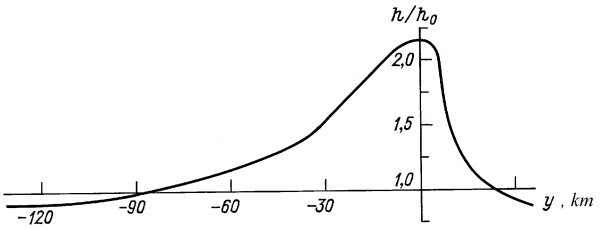

Fig. 6. Distribution of relative mean wave height across current.

The Agulhas current is diverged in a fan-shaped manner at more southern latitudes, becoming weaker. It can be assumed that in the case $x > 0$, the horizontal current velocity components $\boldsymbol{V} = \{V_x(x, y), V_y(x, y)\}$, satisfying the water flux continuity equation, are approximated by the equations:

$$V_x = \frac{b_1}{(1 + b_2 y^2)(1 + b_3 x^2)}, \qquad V_y = \frac{2 b_1 b_3 x}{(1 + b_3 x^2)\sqrt{b_2}} \arctan(\sqrt{b_2} y), \tag{1.2}$$

where $b_3 = 0.6 \times 10^{-11}\ \mathrm{m}^{-2}$.

The swell propagation from southern latitudes, with actually no currents, towards the increasing Agulhas current should be considered. The geometric optics approximation can be applied in this case, because typical horizontal scales of current velocity variations exceed significantly the horizontal wave dimensions. At greater distance from the investigated area (see Fig. 1), the initial spectrum $S_0(\omega, \beta_0)$ is assumed to be prescribed at $x > 1.5 \times 10^6$ m, where the current speed can be neglected: $\sqrt{V_x^2 + V_y^2} \approx 0$. The spectrum can be described with the help of the swell spectrum approximation [8] with $n = 5$, $\omega_{\max} = 0.5\ \mathrm{rad\,s}^{-1}$. It should be noted that the initial value of the angle β_0 included in $S_0(\omega, \beta_0)$ is a function of the values ω, β and the co-ordinates $\{x, y\}$.

In order to find β_0, it is necessary to solve a set of the Hamilton equations, which can be written using new variables:

$$\begin{aligned}
&\frac{\mathrm{d}y}{\mathrm{d}x} = \frac{2V_y + f \sin\beta}{2V_x - f \sin\beta},\\
&\frac{\mathrm{d}\beta}{\mathrm{d}x} = \frac{(\partial V_x/\partial x)\sin 2\beta - (\partial V_y/\partial x)\sin^2\beta + (\partial V_x/\partial y)\cos^2\beta}{V_y - 0.5 f \cos\beta},\\
&\frac{\mathrm{d}t}{\mathrm{d}x} = \frac{2}{2V_y - f\cos\beta}.
\end{aligned} \tag{1.3}$$

where

$$f = \frac{g}{2\omega}\left\{1 + \sqrt{4 - \frac{\sqrt{V_x^2 + V_y^2}}{g}\omega\cos\left(\beta + \arcsin\left(\frac{V_y}{\sqrt{V_x^2 + V_y^2}}\right)\right)}\right\}.$$

The Runge–Kutta method is used to solve set of Eqs. (1.3) for a discrete set of the frequencies ω_1 (from $\omega_1 = 0.37\ \mathrm{rad\,s}^{-1}$ to $\omega_{12} = 0.981\ \mathrm{rad\,s}^{-1}$) and the angles β_j (from -75 to 75° with a step of 15°). Thus, the values β_{0j} are obtained. They correspond to the rays arriving to the given points $\{x = 0, y = y_n\}$ from the region with practically no current $x > 1.5 \times 10^6$ m.

Some most typical rays $y = y(x, \omega, \beta)$ arriving to the point $\{x = 0, y = 0\}$ are depicted in Fig. 5. They are characterized by oscillations relative to the axis Ox. The oscillation frequencies are increased with rays approaching the intense current area. A peculiar wave channel (i.e. a waveguide) appears in the current with the wave rays being alternatively reflected from one or other caustics situated on different sides of the current midstream.

The wave spectrum in the current $S(\omega_i, \beta_j, y_n)$ is obtained at $x = 0$ as a result of numerical simulation of Eqs. (1.3), using the spectral solution of the energy balance equation [5,8]:

$$S(\omega, \beta, U(y)) = \frac{16}{(1 + \sqrt{1 - 4U\omega/g\cos\beta})} \frac{S_0(\omega, \beta_0)}{\sqrt{1 - 4U\omega/g\cos\beta}}. \tag{1.4}$$

In order to obtain the total wave energy, the spectrum is integrated numerically over the frequency ω and the angle β. The estimation results (see Fig. 6) are obtained for the relative mean wave height h/h_0 in the current (where h_0 is the initial wave height without any current), whereas values of the co-ordinate y are plotted along the horizontal axis. The value h/h_0 maximum equal to 2.19 is estimated to be in the midstream. The ratio h/h_0 is sharply decreased along the distance to the shoreline. A relative excess of the wave height is not greater than 10 per cent at a distance of $y = 19$ km from the maximum current velocity line. Seaward to the midstream, the relative height h/h_0 is decreased to a lesser extent with a ten-percent wave height excess, occurring at $y = -70$ km. But a reversed case (i.e., $h < h_0$) is even observed at $|y| > 90$ km. The probability of observing abnormal waves is much less in going towards the shore at some distance from the line of maximum velocity with 200 m isobath, than going the same distance from the maximum velocity current in the direction to the open sea.

Thus, the obtained results indicate that the peculiar velocity distribution of the Agulhas current induces refraction of the southwest swell propagating over a wide area of the southwestern Indian Ocean. It leads to that the swell turns towards the current velocity maximum. The swell is trapped, intensified by the countercurrent and localized in the neighborhood of the maximum velocity, propagating along the southeast coast of South Africa. As a result, there is a significant concentration of the wave energy density, i.e. a focusing takes place in the given area resulting in abnormal wave generation.

2. Wave height amplification around caustic due to refraction wave in non-uniform current

Spectral solution obtained above provides estimation of the mean wave height spatial distribution. This solution is space averaged. The wave phase is omitted. That is why it does not describe waveform as it is. In order to solve this problem the diffraction approach can be applied for wind wave transformation in cross velocity shear current.

There are some different methods giving opportunity to estimate the wave diffraction around caustic [9,8]. In the present paper the wave diffraction is estimated with the help of Maslov's method originally applied here for surface gravity waves in non-uniform current. The method is considered as more accurate and universal than others well known ones.

Now the current velocity $\boldsymbol{V}$ is assumed to be directed along the axis Oy with its changes along the coordinate x: $\boldsymbol{V} = \{0;\, V_y(x)\}$. The depth $H = H(x)$ is also changed along this direction (see Fig. 7). Such situation can appear, for example, in the coastal zone with a along shore current or in Agulhas current.

The equation for the wave packet propagation can be written in the following form:

$$\frac{\mathrm{d}x}{\mathrm{d}t} = C_{gx} = C_g \cos(\beta), \qquad \frac{\mathrm{d}y}{\mathrm{d}t} = C_{gy} = C_g \sin(\beta) + V_y, \tag{2.1}$$

$$\frac{\mathrm{d}k_x}{\mathrm{d}t} = \frac{1}{2}\sqrt{\frac{gk}{\mathrm{th}(kH)}}\,\frac{1}{\mathrm{ch}^2(kH)}\,\frac{\mathrm{d}H}{\mathrm{d}x} + k_y\frac{\partial V}{\partial x}, \qquad \frac{\mathrm{d}k_y}{\mathrm{d}t} = 0. \tag{2.2}$$

As it can be seen from the problem formulation, the coordinate y is cyclic. The component k_y of the wave vector $\boldsymbol{k}$ remains constant along a wave packet propagation trajectory. It be can written [8] as:

$$k_y = k\sin(\beta) = k_0 \sin(\beta_0). \tag{2.3}$$

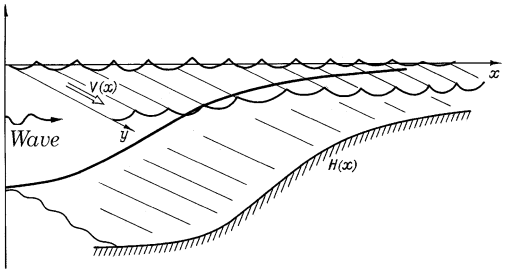

Fig. 7. Wave transformation in a shear horizontally non-uniform current.

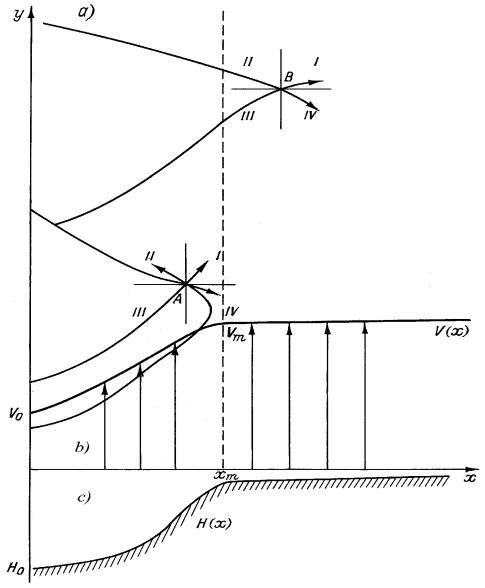

Fig. 8. Trajectories of wave packet propagation against current velocity profile and depth background for different quadrants at points A and B (a); (b) – current velocity profile $V(x)$; (c) – depth change profile $H(x)$.

Trajectories of wave packet propagation against current velocity profile and depth background for different quadrants are presented in Fig. 8.

In order to estimate the wave field around caustic precisely it is necessary to fulfill more accurate calculations than it is made for usual spectral problem solution. For this purpose a modified traditional scheme of the WKB approximation can be applied. In order to do it the Maslov method (Maslov and Fedoryuk [10]), describing the uniform wave field asymptotic in entire space can be used.

The application of the geometrical optics method leads to the amplitude value singularity in the caustic. However, in case the wave field is described by the integral representation the wave amplitude is finite around caustic. The Fourier integral is proposed to be used as a such representation. Integration is made over the wave vector component $\boldsymbol{k}$, in which direction the wave medium properties are changed (for example, along the axis Ox). In other words, describing the wave field one proceeds from the spatial coordinates $\{x_1 = x, x_2 = y\}$ to the mixed spatial-momentum representation $\{k_1 = k_x, x_2 = y\}$. The wave vector component, directed along the axis Oy is constant, i.e. $k_y = k_{y0}$. The frequency ω is persevered [8] along the ray as well:

$$\omega = F(k_x, k_{y0}, x) = Const. \tag{2.4}$$

As it follows from Eqs. (2.1), (2.2), the trajectory of the wave packet propagation can be parametrically presented in the following form:

$$\int_{x_0}^{x} C_{gx}^{-1}\,\mathrm{d}x = t - t_0, \qquad y = y_0 + \int_0^t C_{gy}\,\mathrm{d}t. \tag{2.5}$$

Where the initial data are prescribed as $x|_{t=t_0} = x_0$, $y|_{t=t_0} = y_0$, $k_x|_{t=t_0} = k_{x0}$, $k_y|_{t=t_0} = k_{y0}$. The wave amplitude at the initial moment $a(x, y, t)|_{t=t_0} = a_0$ is also considered to be known.

According to the Maslov method scheme, the wave integral presentation can be written as:

$$\eta(x, y, t) = \frac{1}{\sqrt{2\pi}} \int a_0 \sqrt{\frac{\sigma}{\sigma_0}\left(\frac{\partial(k_x, y)}{\partial(x_0, y_0)}\right)^{-1}}\, \exp\bigl\{\mathrm{i}\bigl[k_x(x - \tilde{x}) + \psi(\tilde{x})\bigr]\bigr\}\,\mathrm{d}k_x, \tag{2.6}$$

where the wave number k_x is the integration variable; $\tilde{x}$ is the function of k_x, obtained from Eq. (2.4) x; $\psi(x, y, t)$ is a usual wave phase. σ, σ_0 are wave frequencies relative to immovable water at the given and initial time moments $t = t_0$.

The Jacobian can be written in (2.6) as follows:

$$\frac{\partial(k_x, y)}{\partial(x_0, y_0)} = \frac{\partial k_x}{\partial x}\frac{\partial(x, y)}{\partial(x_0, y_0)} = \frac{\partial k_x}{\partial x}\frac{\partial x}{\partial x_0}. \tag{2.7}$$

Using (2.4) and (2.5) it can be found out that: $\partial k_x/\partial x = -\partial F/\partial x/C_{gx}$, $\partial x/\partial x_0 = C_{gx}/C_{gx0}$. The integral value (2.6) can be estimated with the help of the saddle-point method. The saddle-point k_x^{**} is found using the equation $\partial\Theta/\partial k_x = 0$, where $\Theta(x, k_x) = k_x(x - \tilde{x}) + \tilde{\psi}(x)$. As soon as $\frac{\partial\Theta}{\partial k_x} = x - \tilde{x} + (\partial\psi/\partial\tilde{x} - k_x)(\partial k_x/\partial x) = x - \tilde{x}$, it turns out that $\tilde{x}(k_x^{**}) = x$ and $\partial^2\Theta/\partial k_x^2 = -\partial\tilde{x}/\partial k_x = C_{gx}/(\partial F/\partial x)$. An application of the usual saddle-point method to the integral (2.6) leads to the following formula:

$$\eta(x, y, t) = a_0\sqrt{\frac{\sigma}{\sigma_0}\frac{C_{gx0}}{C_{gx}}}\,\exp\{\mathrm{i}\psi\}. \tag{2.8}$$

The insignificant phase factor is omitted in this ratio. The expression (2.8) makes up a condition of the wave action density preservation.

Now the "turning" point of $x = x^*$ should be considered. A sign of the velocity C_{gx} is changed, and the wave packet propagation begins moving to the opposite direction at this point. In this case: $\partial^2\Theta/\partial k_x^2|_{k=k*} = 0$, and the phase expansion $\Theta(k_x)$ starts with the term of order $(k_x - k_x^*)^3$ at the saddle-point $k_x^{**} = k_x^*$:

$$\left.\frac{\partial^3\Theta}{\partial k_x^3}\right|_{x=x^*} = \left.\frac{\partial}{\partial k}\left(\frac{C_{gx}}{\partial F/\partial x}\right)\right|_{x=x^*} = \left.\frac{1}{\partial F/\partial x}\frac{\partial C_{gx}}{\partial k_x}\right|_{x=x^*}. \tag{2.9}$$

Considering some area around the turning point $x = x^*$, with the saddle-point k_x^{**} being close to k_x^*, the expression for $\Theta(k_x)$ can be restricted with the terms of $(k_x - k_x^*)^3$ order. The asymptotic expression can obtained using such expansion of the integral (2.6) and omitting the insignificant phase factor:

$$\eta(x, y, t) = a_0 \sqrt{2\pi \frac{\sigma}{\sigma_0} \frac{C_{gx}}{\partial F/\partial x}}\, \kappa^* Ai\Big[\kappa^*(x - x^*)\Big] \exp\big\{i\big[k_x^*(x - x^*) + \psi(x^*)\big]\big\}, \tag{2.10}$$

where $Ai(X)$ is the Airy function,

$$\kappa^* = \left[\frac{1}{2} \frac{1}{\partial F/\partial x} \frac{\partial^2 F}{\partial k_x^2}\right]^{-1/3}\Bigg|_{x=x^*}.$$

The Airy function $Ai(X)$ is estimated for the large positive values ($X > 0$) as:

$$Ai \approx \frac{1}{\sqrt{2\pi}} X^{-1/4} \exp\left(-\frac{2}{3} X^{3/2}\right), \tag{2.11a}$$

and for the large negative values ($X < 0$) as:

$$Ai \approx \frac{1}{\sqrt{2\pi}} X^{-1/4} \cos\left(\frac{2}{3} |X|^{3/2} - \frac{\pi}{4}\right). \tag{2.11b}$$

The Airy function can be presented at $X < 0$ as a superposition of two exponential functions as $\exp(\pm iX)$, one of them describing the straight and the second the reflected waves. These two waves with close wave numbers superimposing each other create the interference pattern, with total amplitude subjected to modulation containing an area with very large amplitudes of surface elevation.

A wave vector component is defined as $k_x = k_x^* \pm \sqrt{\kappa^{*3}(x^* - x)}$ in the vicinity of the turning point. The $(\pm)$ signs are referred to the straight and reflected waves, respectively. There is a shift by $-\pi/2$ in the reflected wave phase due to the ray touching the caustic. Taking into account the latter ratio in the formula (2.8), as well as applying asymptotic of the Airy function (at $X < 0$) in the formula (2.10), the results are coincided, indicating the uniformity of the asymptotic solution. The solution around the caustic with asymptotic is shown in Fig. 9.

The maximum amplitude $a = |\eta|$ is reached with $\kappa^*(x^* - x) = 1.02$; at the same time $Ai = 0.536$.

$$a_{\max} \cong 1.69 a_0 \sqrt{\frac{\sigma}{\sigma_0} C_{gx}} \left|\frac{\partial F}{\partial x}\right|^{-\frac{1}{6}} \left(\frac{\partial^2 F}{\partial k_x^2}\right)^{-1/3}\Bigg|_{x=x^*}, \tag{2.12}$$

$$\frac{\partial F}{\partial x} = k_y \frac{\partial V}{\partial x}, \qquad \frac{\partial^2 F}{\partial k_x^2} = \frac{1}{2}\sqrt{g/k^3}\left(1 - \frac{3}{2} k_x^2 k^{-2}\right). \tag{2.13}$$

At the turning point $x = x^*$ the following values are defined as

$$\kappa_* = \frac{1}{2}\left(\frac{\partial F}{\partial x}\sqrt{\frac{\partial^2 F}{\partial^2 k_x}}\right)^{-1}\Bigg|_{x=x^*}, \quad C_{gx} = 0, \quad k_x = k_x^* = 0, \quad \sigma^*/\sigma_0 = \sqrt{k_x/k_0}.$$

A substitution of these relations to the asymptotic expression (2.6) results in the following free surface elevation:

$$\eta = a_0 \sqrt[3]{4}\sqrt{\pi \cos(\beta_0)}\big(\sin(\beta_0)\big)^{7/12}\left(\sigma_0 \frac{\partial V}{\partial x}\right)^{1/6}\Bigg|_{x=x^*} Ai\big[\kappa_*(x - x^*)\big] \exp\big[ik_x(x - x^*) + i\psi(x^*)\big]. \tag{2.14}$$

Using this formula it is easy to find out the amplitude maximum, taking place at $\kappa_*(x - x^*) = 1.02$ for the initial angle $\beta_0 = 42.79°$:

$$a_{\max} = 1.04 a_0 \left(\frac{\sigma_0}{\partial V/\partial x}\right)^{1/6}. \tag{2.15}$$

It should be noted that the expression (2.15) coincides with the earlier derived ratio [9], with an exception that the value $\sigma|_{x=x^*} = \sqrt{gk_y}$ is used instead of σ_0. As a result, the amplitude maximum is achieved at $\beta_0 = 45°$, and the numerical coefficient in the expression (2.15) makes up 1.065 (instead of $\beta_0 = \arccos(\sqrt{7/13}) = 42.79°$ and the coefficient of 1.04).

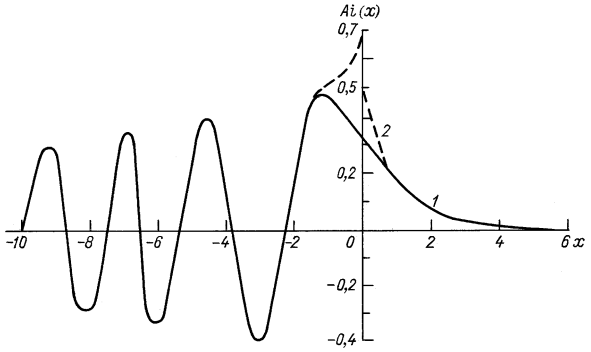

Fig. 9. Airy function and its asymptotic approximations (2.11a) for $X > 0$ and (2.11b) for $X < 0$.

As an example a swell height increase in field condition should be estimated. Thus, if the wavelength is equal to 50 m. and the velocity gradient is $\Delta V/\Delta x = 10^{-4}$, then the swell height increase is equal to ≈ 4.64. The wave steepness around the caustic can be easily determined using the expressions (2.3), and (2.15) as:

$$a_{\max}k^* = 1.51a_0k_0\big(\cos(\beta_0)\big)^{19/12}\big(\sin(\beta_0)\big)^{1/2}\left(\frac{\sigma_0}{\partial V/\partial x}\right)^{1/6}\Bigg|_{x=x^*}. \tag{2.16}$$

The maximum of this value is achieved at $\beta_0 = 31.255^\circ$ and it is equal to:

$$(ak)_{\max} = 0.848a_0k_0\left(\frac{\sigma_0}{\partial V/\partial x}\right)^{1/6}\Bigg|_{x=x^*}. \tag{2.17}$$

Thus, there is strong impact current on wave field around caustic. It can produce amplitude modulation, large wave height amplification up to 4.6, and wave steepness up to 3.8 due to wave length variation.

3. Non-linear wave interaction in shallow water due to their intersection described by the Kadomtsev–Petviashvili equation

Another important current impact on the wave evolution may happen not in a caustic area located at the large current speed gradient, but in the middle part of the current where intersection of waves moving from different directions reflected by current (Fig. 5). It is shown in [11] that specific mechanism may become evident if the evolution of the long-wave in this case is described by the Kadomtsev–Petviashvili (KP) equation. It should be noted that for the first time such mechanism of freak wave generation was discussed in Prof. T. Soomere [12].

Let us consider the reasons in favor of the long-wave shallow water consideration taking into account the case shown in Fig. 2. The data are taken from [2,5], where it is noted that the ship is lowered down on the long forerunner (or sloping trough) before the rogue wave affects it, see Fig. 2. Likely the forerunner is a part of the rogue wave hence one can suggest that the typical horizontal size, L, of the wave lies in the interval $L \approx 500$ m or the double ship length. The depth of the ocean, H, according to [2,5] is $H = 200$ m, while the amplitude of the wave, A, is $A = 20$ m. The relationships, $A/H = 0.1$ and $H/L = 0.33$, satisfy the shallow water theory, see, e.g., [13,14]. Moreover, $A/H = \mathrm{O}(H^2/L^2)$, that corresponds to the balance between nonlinearity and dispersion.

Also observations demonstrate us that perhaps the rogue wave is a two-dimensional localized or solitary wave. Transverse variation of the horizontal speed of the Agulhas current may be responsible for the transverse localization of the wave. One can see from Figs. 4, 6 that typical size of the transverse current variation, Y, is equal to several kilometers. Then the relationship is of order of, $L/Y = \mathrm{O}(H/L)$, and the transverse variations are weaker than those along the current.

Let us consider the ocean as an inviscid liquid layer of permanent depth H while the influence of the open air is negligibly small. Assume the plane $z = 0$ of the Cartesian coordinates coincides with undisturbed free surface of the layer, hence fluid occupies the region $-H < z < \eta$, $\eta(x, y, t)$ is a free surface disturbance. Let us denote the liquid density by ρ, velocity components along axes x, y, z by $u(x, y, z, t)$, $v(x, y, z, t)$ and $\omega(x, y, z, t)$ respectively. Let t is time, p is pressure.

As usual, it is convenient to introduce the velocity potential, $u = \Phi_x$, $v = \Phi_y$ and $\omega = \Phi_z$.

Following the scaling analysis, we shall consider the long waves with small but finite amplitude. Then the scales are introduced as follows: L for x, Y for y, H for z, $L/\sqrt{gH}$ for t, A for η, and $AL/H\sqrt{gH}$ for Φ. The small parameter of the problem, ε, is

$$\varepsilon = A/H = H^2/L^2,$$

also it is assumed that $L/Y = \sqrt{\varepsilon}$. Introducing the phase variable $\theta = x - t$ and the slow time $\tau = \varepsilon t$, one can obtain from the last equations the well known Kadomtsev–Petviashvili (KP) equation [13,14] for the function, $\eta = \phi_\theta$,

$$(2\eta_\tau + 3\eta\eta_\theta + 1/3\eta_{\theta\theta\theta\theta})_\theta + \eta_{yy} = 0. \tag{3.1}$$

Well-known plane solitary wave solution of Eq. (3.1) [13,14] may be written in dimensional form as

$$\eta = \frac{4Ak^2}{3}\cosh^{-2}\frac{k}{L}\left(x + m\frac{mL}{Y}y - \sqrt{gH}\left(1 + \frac{A}{H}\frac{3m^2 + k^2}{6}\right)t\right). \tag{3.2}$$

This solution is localized only along the direction of propagation, while another exact two-dimensional localized traveling wave solution requires an opposite sign at η_{yy} or at $\eta_{\theta\theta\theta\theta}$ [13–15]. In our case the negative sign at the dispersion term in Eq. (3.8) may be formally achieved if the surface tension is taken into account. Then the coefficient is changed from $1/3$ to $1/3 - Bo^{-1}$, where the Bond number, $Bo = \rho g H^2/\sigma$, σ is the surface tension coefficient. Its sign may be negative if the Bond number is less than 3, that happens only for thin liquid films [16,17] but not in the ocean.

The KP equation also possesses two-solitary wave solution [13],

$$\eta = \frac{4}{3}\frac{\partial^2}{\partial\theta^2}\log(F), \qquad F = 1 + \exp(\xi_1) + \exp(\xi_2) + \exp(A_{12} + \xi_1 + \xi_2),$$
$$\xi_i = k_i\left(\theta + m_i y - \frac{3m_i^2 + k_i^2}{6}\tau\right), \qquad \exp A_{12} = \frac{(k_1 - k_2)^2 - (m_1 - m_2)^2}{(k_1 + k_2)^2 - (m_1 - m_2)^2}. \tag{3.3}$$

Its typical shape is shown in Fig. 10. One can see a localized structure in the area of the waves interaction. It moves keeping its shape and velocity, and the amplitude is four times higher than the amplitude of single solitary wave [4,18]. This solution does not describe a formation of localized wave. That is why initial conditions for numerical simulations were used in [11] in the form of the semi-plane solitary waves without interaction area. It was found that the incident waves may be considerably deformed after the interaction, and there arise a steady two-dimensional localized wave moving along the x-axis, see Fig. 11. To some extent, the shape of the stem is similar to the localized structure shown in the centre of Fig. 10, and possible largest amplitude of the stem wave is almost four times greater than the amplitude of the incident wave (not the sum of them). The largest amplitude is achieved when the angle between interacting plane solitary waves lies in a certain, rather narrow, interval, see Fig. 12. In dimensional variables

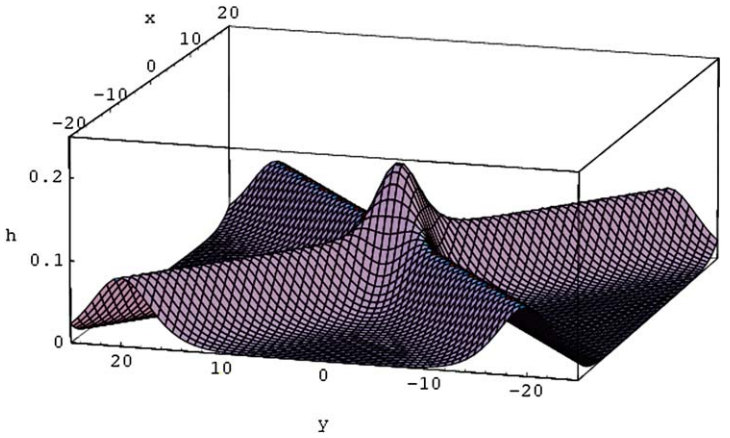

Fig. 10. Interaction of the plane solitary waves described by the KP two-solitary waves.

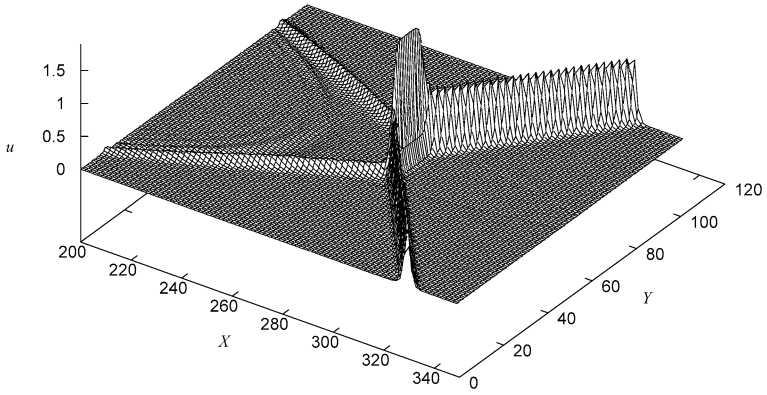

Fig. 11. Two-dimensional localized wave or a stem.

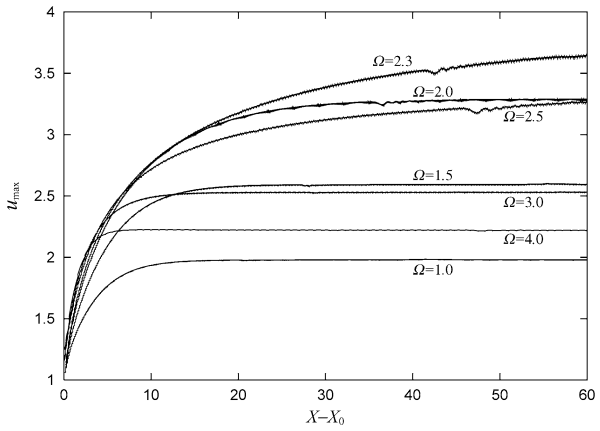

Fig. 12. Dependence of the stem amplitude on the angle Ω (rad) between incident waves.

in our case it is equal to 15–20 degrees. Dimensional estimations done in [11] show that the stem is generated within 4 min for certain realistic initial conditions that may be a reason why an abnormally high wave appears suddenly for the crew of a vessel. The features of the wave are found to be closer to the single plane solitary wave solution rather than to the two-solitary wave solution studied thoroughly in [19]. Also it was found that the curvature of the initial semi-infinite waves affects the higher amplification of the wave. In particular, calculations demonstrate an increase in the wave amplitude up to 14 times at certain conditions, see [11] for details. The last wave is unstable, it exists for a short time but sufficient to attack a vessel found itself in the place of the wave appearance.

All above mentioned waves are the waves of elevation. One can suggest that the wave with a deep trough may appear if the initial curved waves are the waves of depression. Of course the KP equation (3.1) does not support stable propagation of solitary waves with negative amplitude, however, a short time evidence of higher amplitude localized wave might be possible, this problem will be studied in the nearest future.

4. Conclusion

The term ‘freak waves’ (or abnormal waves) pertains to individual waves with a crest of an extremely high slope, in front of which there appears a longer and deeper trough than compared with ordinary wind waves. It is rather difficult to observe a hole at some distance from a ship. That is why it is practically impossible for a ship’s crew to take any precaution measures. Abnormal waves are observed frequently in different regions of the world ocean with strong currents such as Gulfstream, Kuroshio and others. Extremely large waves are observed near the southeastern shore of South Africa in the Agulhas current between East London and Durban.

There are at least three reasons for freak wave generation due to wave interaction with non-uniform current.

- Wave energy amplification due to wave-current interaction;
- Wave height amplification around caustic due to refraction wave in non-uniform current;
- Non-linear wave interaction in shallow water due to their intersection described by the Kadomtsev–Petviashvili equation.

The mutual relation and joint importance of the three mechanisms discussed in the paper. It is shown that remarkable wave energy concentration may happen in the mid-stream of strong spatially inhomogeneous currents. It may lead to general increase of wave height in some region. In the peripheral area of such currents another mechanism may produce abnormally high wave groups, surface elevation in which are describe by the Airy function. At top of all that, intersection of long-crested wave packets, reflected or refracted in a proper manner by the current (and possibly having curved fronts owing to refraction due to local inhomogeneities of the current) may result in both short- and long-living extremely high wave humps all over the area of spatially varying current.

Acknowledgements

One of the authors (IVL) acknowledges the support of the Russian Foundation for Basic Researches under the grant No. 05-05-08027 ofi-a. The authors thank Professor H. Moes for the donation of the data, which is used for preparation of Fig. 3, and Prof. T. Soomere and Yu. Stepanyants for fruitful discussions and valuable comments.

References

[1] J.K. Mallory, Normal waves on the south-east of South Africa, Inst. Hydrog. Rev. 51 (1974) 89–129.
[2] I.V. Lavrenov, Ship collision with “freak-wave”, Marine Fleet 12 (1985) 28–30 (in Russian).
[3] H. Moes, Presentation at MaxWave Project Concluding Symposium, Geneva, 8–12 October, 2003.
[4] C. Kharif, E. Pelinovsky, Physical mechanisms of the rogue wave phenomenon, Eur. J. Mech. B Fluids 22 (2003) 603–635.
[5] I.V. Lavrenov, The wave energy concentration at the Agulhas current of South Africa, Natural Hazards 17 (1998) 117–127.
[6] A.A. Kurkin, E.N. Pelinovsky, Freak Waves: Facts, Theory and Modelling, Nizhny Novgorod State Technical University, Ministry of Education of the Russian Federation, Nizhny Novgorod, 2004 (in Russian, 158 p).
[7] E.H. Schuman, High waves in the Agulhas curren, Mariners Weather 20 (1) (1976) 1–5.
[8] I.V. Lavrenov, Wind Waves in Ocean, Springer, Berlin, 2003.
[9] D.H. Peregrine, Interaction of water waves and currents, in: Advances in Applied Mechanics, vol. 16, 1976, pp. 10–117.
[10] V.P. Maslov, M.V. Fedoryuk, Quasi-Classical Approximation for Quantum Mechanics Equations, Nauka, Moscow, 1976 (in Russian).
[11] A.V. Porubov, H. Tsuji, I.V. Lavrenov, M. Oikawa, Formation of the rogue wave due to nonlinear two-dimensional waves interaction, Wave Motion 42 (3) (2005) 202–210.
[12] T. Soomere, Personal communication, Vienna, EGU, 2005.
[13] M. Ablowitz, H. Segur, Solitons and Inverse Scattering Transform, SIAM, Philadelphia, 1981.
[14] B.B. Kadomtsev, V.I. Petviashvili, The stability of solitary waves in a weakly dispersive media, Sov. Phys. Dokl. 15 (1970) 539–541.
[15] D.E. Pelinovsky, Yu.A. Stepanyants, Solitary wave instability in the positive-dispersion media described by the two-dimensional Boussinesq equations, JETP 79 (1994) 105–112.
[16] L.A. Abramyan, Yu.A. Stepanyants, The structure of two-dimensional solitons in media with anomalously small dispersion, Sov. Phys. JETP 61 (1985) 963–966.
[17] Y.A. Stepanyants, Dispersion of long gravity-capillary surface waves and asymptotic equations for solitons, Proc. Russ. Acad. Eng. Sci. Ser. Appl. Math. Mech. 12 (2005) 33–40 (in Russian).
[18] T. Soomere, Interaction of Kadomtsev–Petviashvili solitons with unequal amplitudes, Phys. Lett. A 332 (2004) 74–81.
[19] P. Peterson, T. Soomere, J. Engelbrecht, E. van Groesen, Soliton interaction as a possible model for extreme waves in shallow water, Nonlinear Process Geophys. 10 (2003) 503–510.